Chaotic mixing of yield stress materials

Teodor Burghelea

Chaotic mixing of yield stress materials

Teodor Burghelea

PII: S2772-5693(22)00107-4

DOI: https://doi.org/10.1016/j.sctalk.2022.100107

Reference: SCTALK 100107

To appear in:

Please cite this article as: T. Burghelea, Chaotic mixing of yield stress materials, (2022), https://doi.org/10.1016/j.sctalk.2022.100107

Chaotic mixing of yield stress materials

Teodor Burghelea
Nantes Université, CNRS, Laboratoire de Thermique et Energie de Nantes, UMR 6607, La Chantrerie, Rue Christian Pauc, B.P. 50609, F-44306 Nantes Cedex 3, France
Corresponding M **email address and Twitter handle**
Teodor.Burghelea@univ-nantes.fr

Abstract
Pasty materials academically referred to as "yield stress" materials are ubiquitous in daily life whether we think of food products (e. g. mayonnaise, mustard, ketchup etc.), beauty products (e.g. hand creams, hair gels, shower gels etc.), construction materials (cement, mud) or we try to understand the geophysical scale dynamics of volcanic magmas and land-slides. A key issue that has been little (or not at all) addressed so far is rather basic and may be shortly phrased as *"'How do we mix such materials?"* which sets up the global aim of the present contribution. To address this issue, I will first reveal a catastrophic failure of the mixing by the laminar chaotic advection induced by the presence of the yield stress. Next, I will dwell deeper into the physical reasons underlying this fact in terms of both a systematic Eulerian frame and a systematic Lagrangian frame analysis. As a key finding, I will show a clear departure of the spectra of fluctuations of the passive scalar from the analytical prediction proposed by G. K. Batchelor for a temporarily random and spatially smooth flow in terms of the emergence of a spectral peak that blocks the passive scalar cascade. The additional space scale related to the position of the spectral peak is related to the characteristic size of un-yielded materials. Finally, I will discuss two simple solutions able to alleviate to some extent the loss of mixing without paying a hefty energetic price.
Keywords
yield stress materials, laminar chaotic advection, mixing, Finite Time Lyapunov exponents

Figures and tables

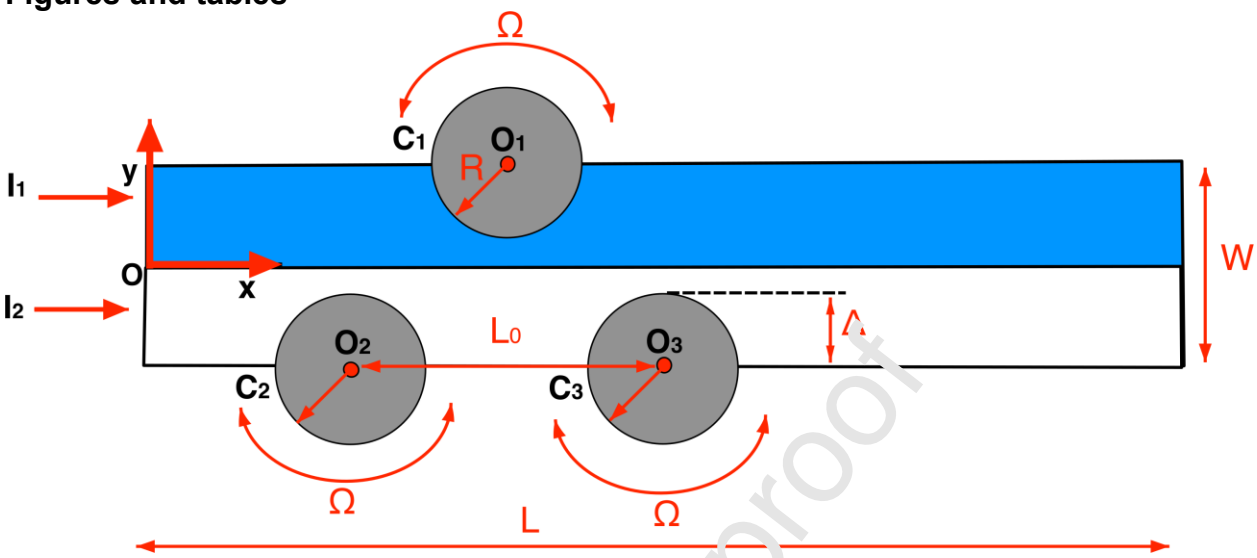

Figure 1. Schematic representation of the channel equipped with three rotating arc-walls (in scale).

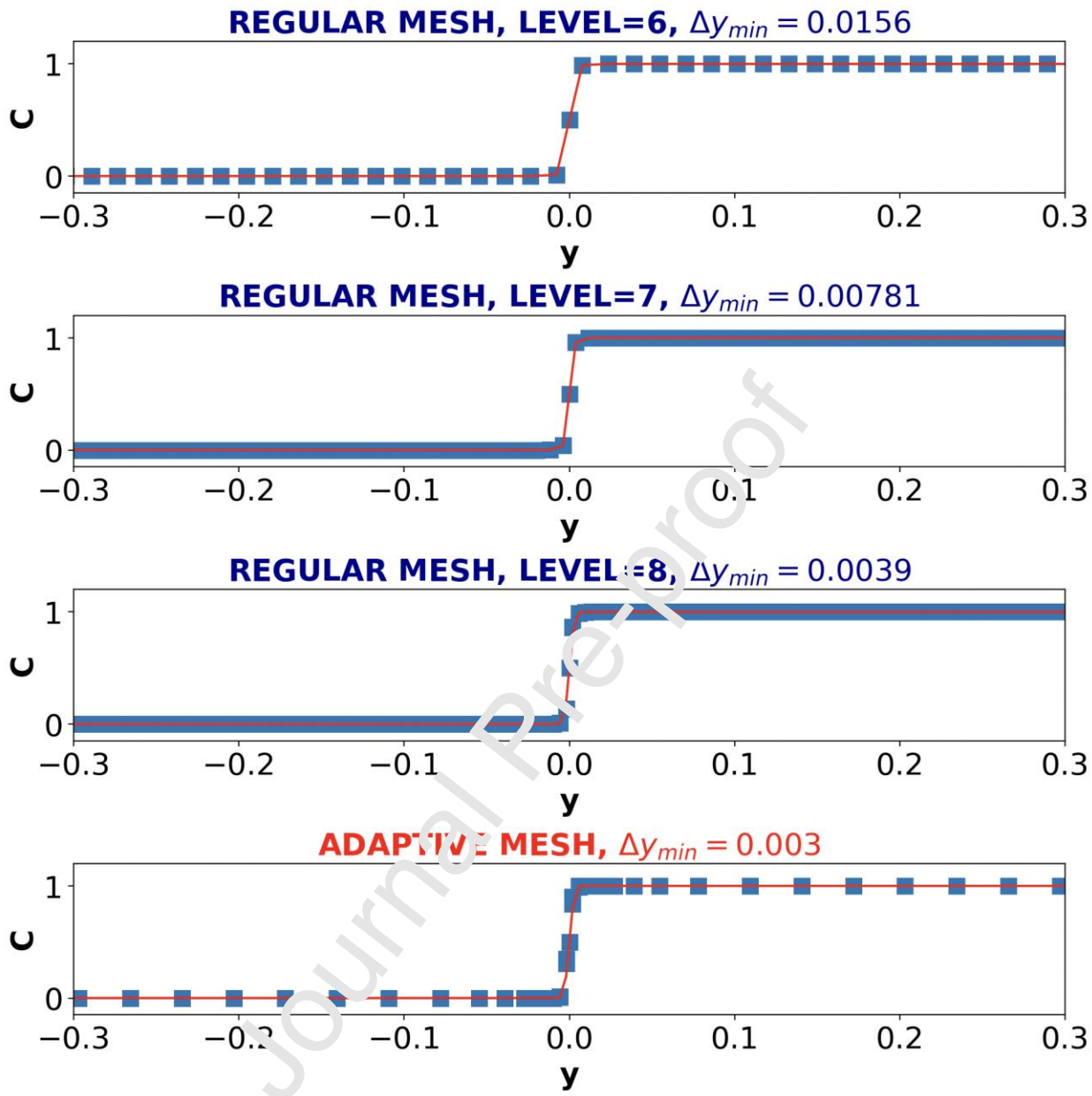

Figure 2. Transverse profiles of the passive scalar concentration C at the exit of the mixer obtained for various values of the spacing Δy_{min} indicated in the top insets. The last case illustrated in the bottom panel refers to the adaptive meshing technique - see text for description. The full lines in each panel are nonlinear fitting functions according to the analytical solution.

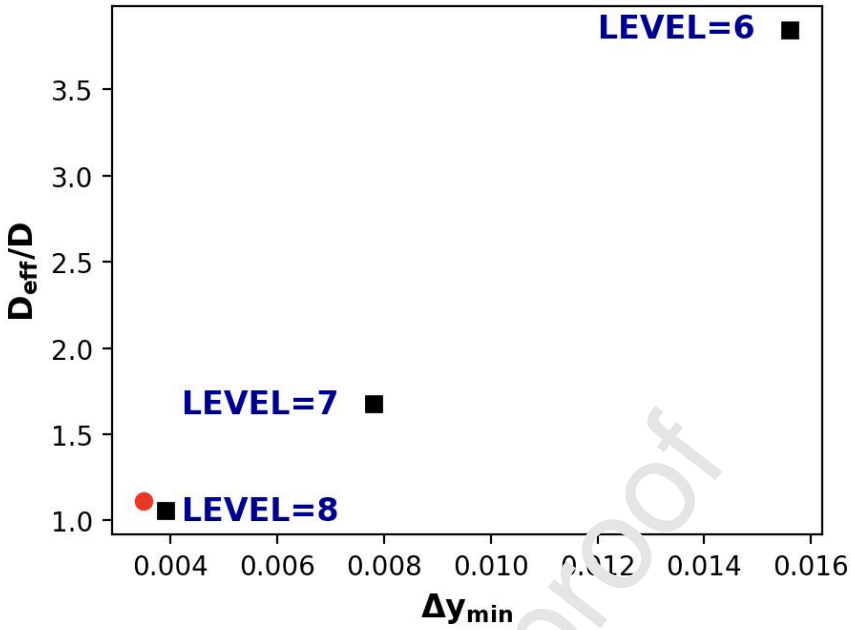

Figure 3. Dependence of the effective diffusion coefficient normalized by the molecular diffusion coefficient D_{eff}/D on the mesh size in the vicinity of y_{min} computed for regular mesh (black squares) obtained from the data sets presented in the top three sub-panels of Fig. 2 and the adaptive mesh (red circle) obtained from the data set presented in the bottom panel of Fig. 2.

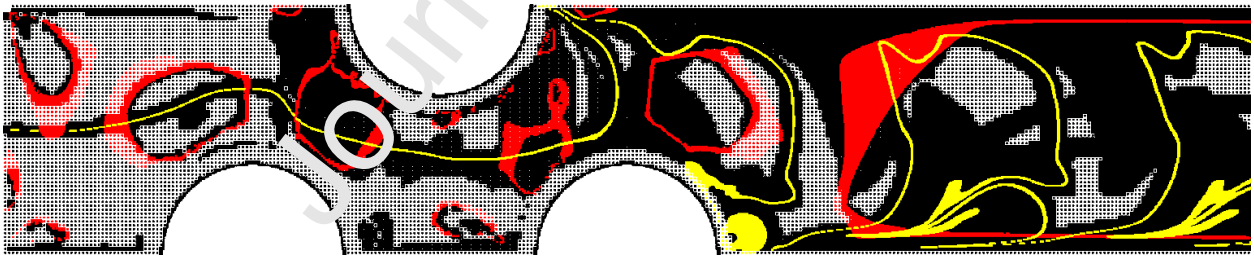

Figure 4. Illustration of the adaptive grid during a simulation of the mixing process at large bulk Bingham number, Bn_{bulk} = 26.5. The dense grid points coloured in yellow mark the interface of the passive scalar while those marked in red mark the yield surface (see text for description). The dense black grid points have resulted from the vorticity based dynamic mesh adaptivity.

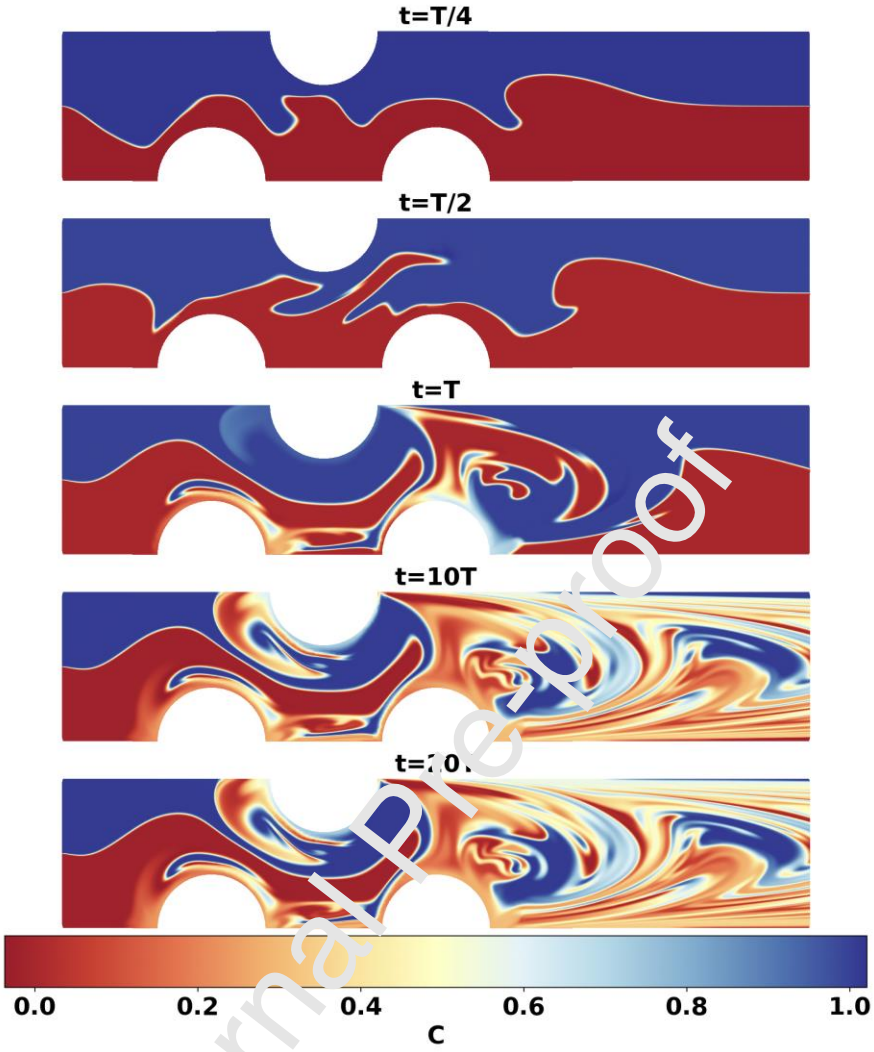

Figure 5. Mixing patterns for the Newtonian case (Bn_{bulk} = 0, N = 1) at several time instants indicated in the top inserts.

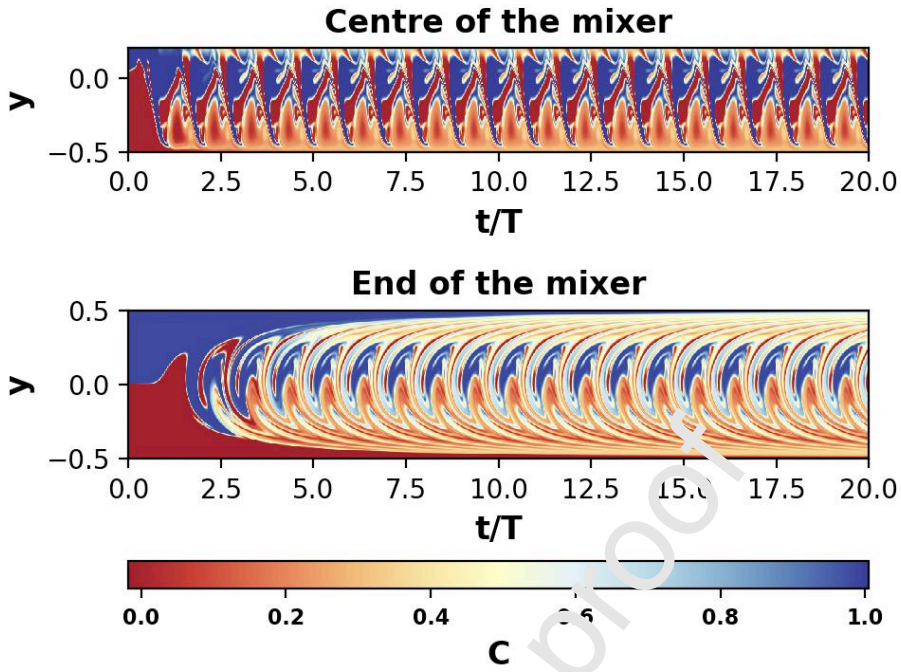

Figure 6. Space time plots obtained for the Newtonian case (Bn_{bulk} = 0, N = 1) at the centre of the mixer (top panel) and at the exit of the mixer (bottom panel).

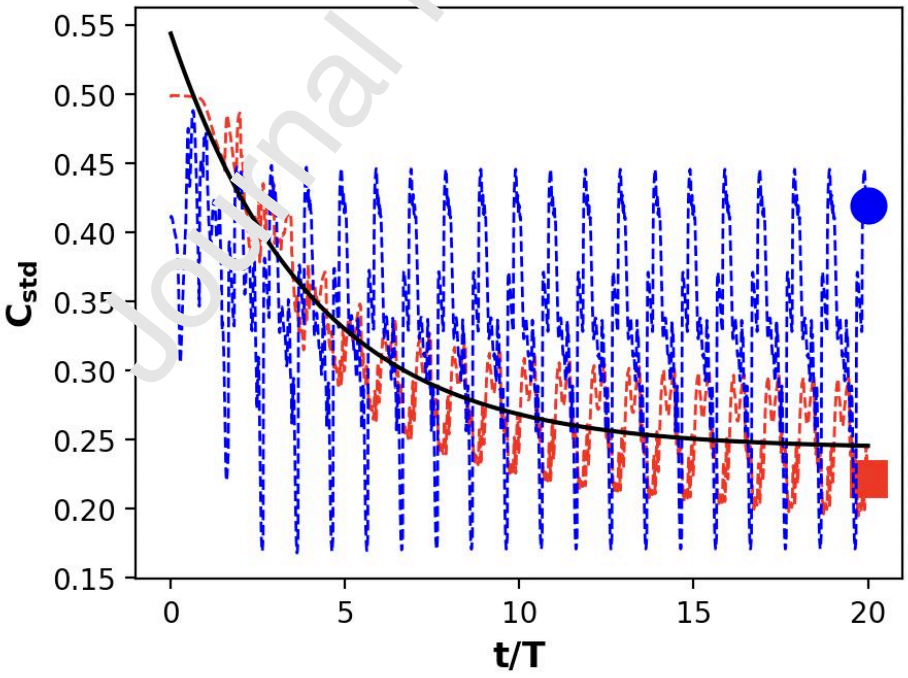

Figure 7. Time series of the mixing indicator C_{std} obtained for the Newtonian case (Bn_{bulk} = 0, N = 1) at the centre of the mixer (circle) and at the exit of the mixer (square). The full line is an exponential fitting function.

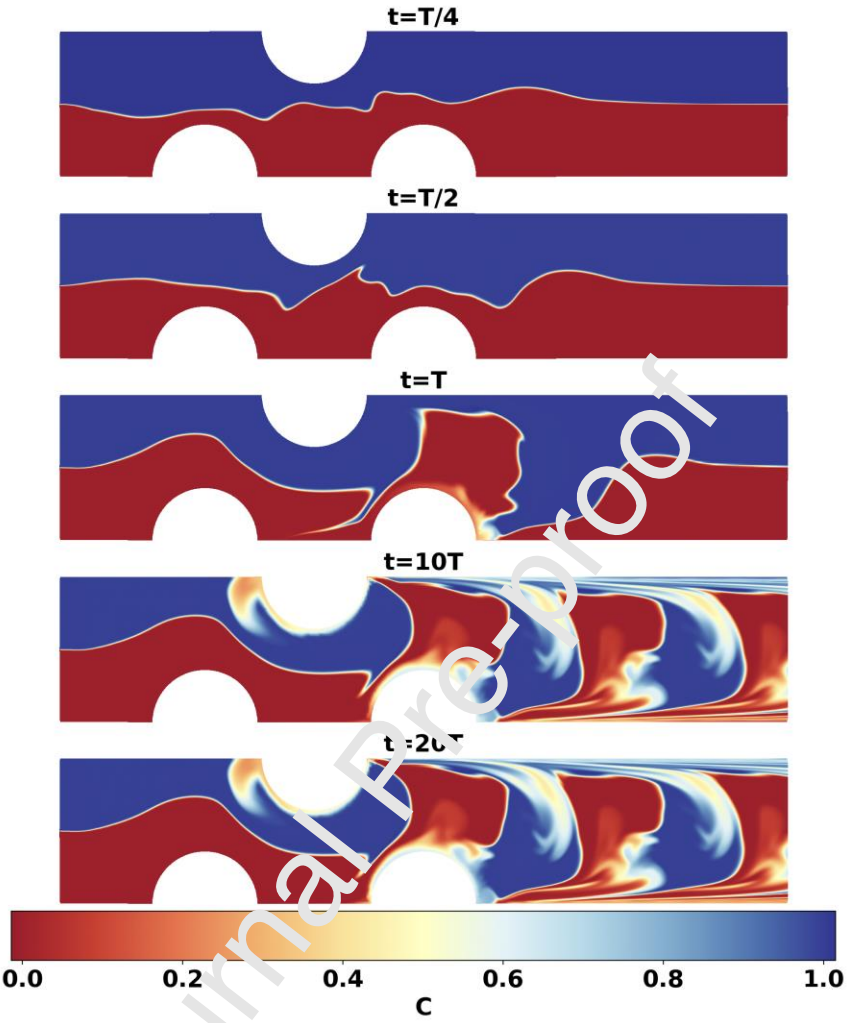

Figure 8. Mixing patterns for largest yield stress explored (Bn_{bulk} = 26.5, N = 0.75) at several time instants indicated in the top inserts.

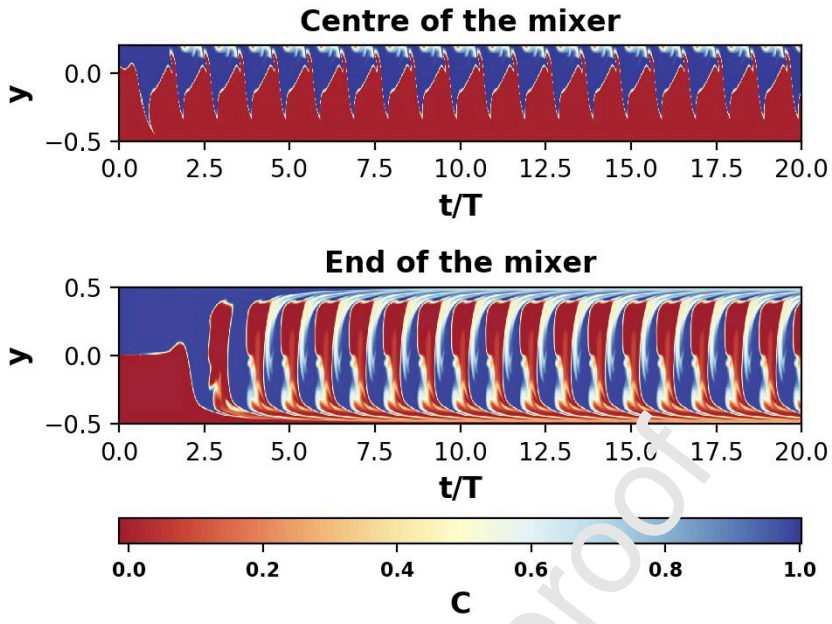

Figure 9. Space time plots of the passive scalar C obtained for the highest yield stress case (Bn_{bulk} = 26.5, N = 0.75) at the centre of the mixer (top panel) and at the exit of the mixer (bottom panel).

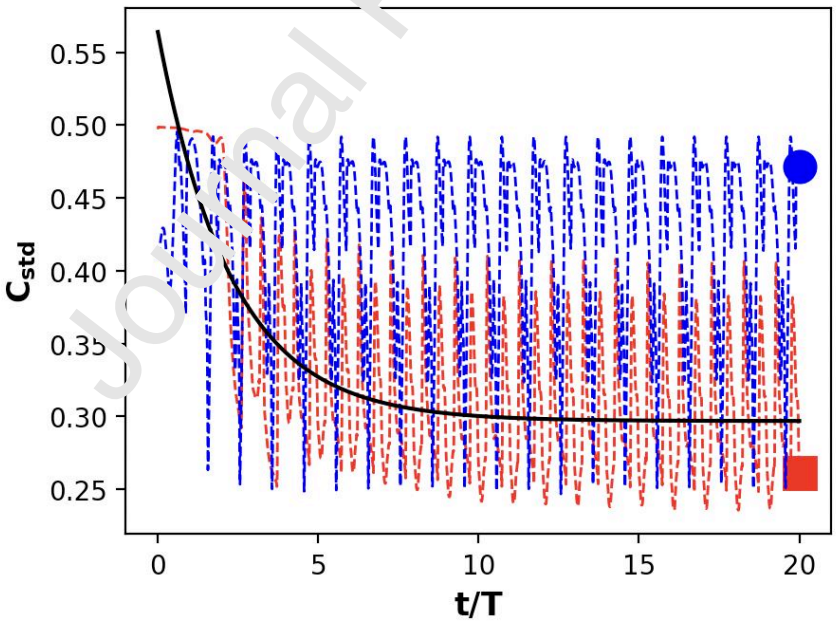

Figure 10. Time series of the mixing indicator C_{std} obtained for the highest yield stress case (Bn_{bulk} = 26.5, N = 0.75) at the centre of the mixer (circle) and at the exit of the mixer (square). The full line illustrates a failed attempt to fit exponentially the time series of the mixing indicator at the channel exit.

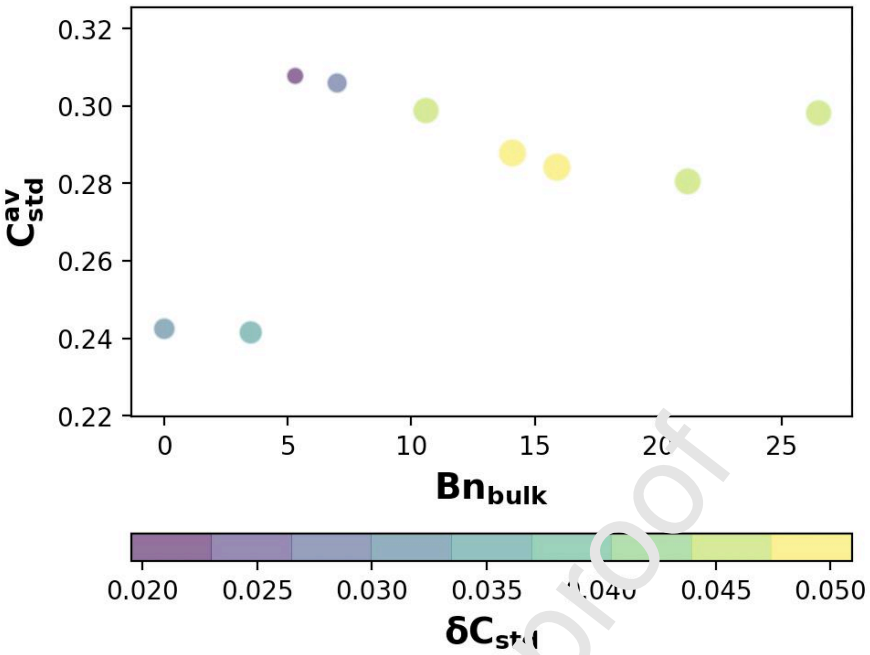

Figure 11. Dependence of the mixing efficiency defined as the variance of the passive scalar concentration at the exit of the mixer, C_{std}, on the bulk Bingham number Bn_{bulk}. Both the color and the relative size of the symbols indicate the value of C_{std} around its dynamical steady state value.

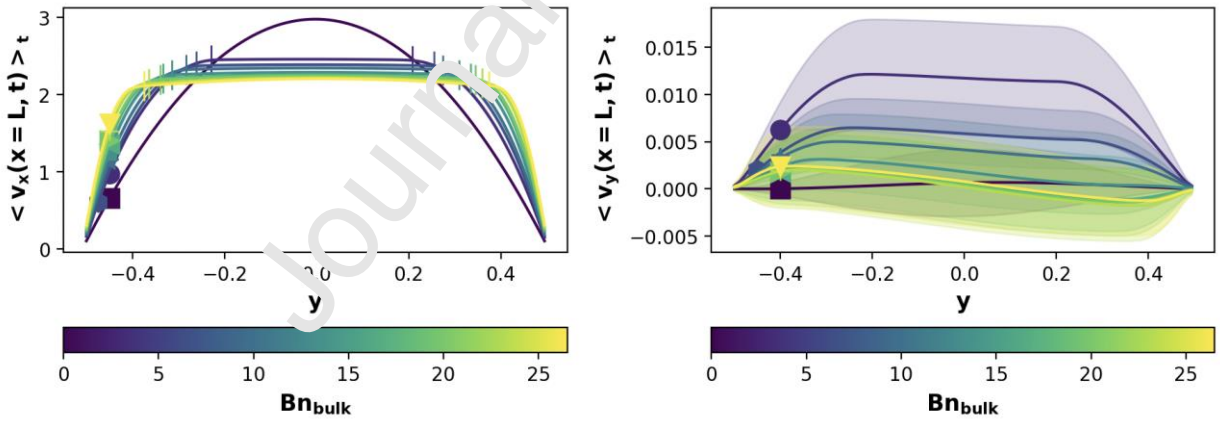

Figure 12. LEFT: Time averaged transverse profiles of the axial velocity; RIGHT: Time averaged transverse profiles of the transverse velocity.

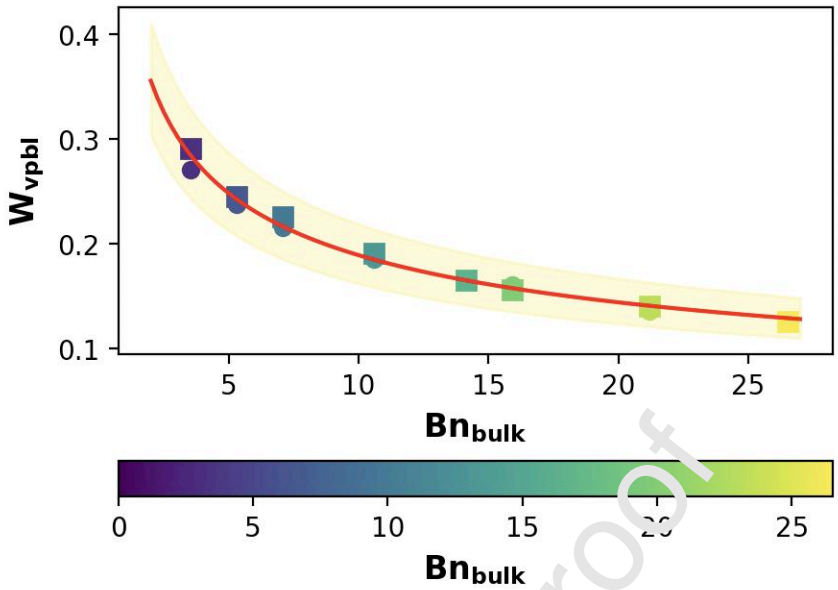

Figure 13. Dependence of the width of the yielded zones (or viscoplastic boundary layers) observed at the channel outlet on the bulk Bingham number Bn_{bulk}. The full line is a power law fitting function, $Bn_{bulk}^{-0.39\pm0.015}$. The shaded area highlights the bulk confidence bounds of the power law fit. In each subplot the colorbar maps indicates the value of Bnbulk.

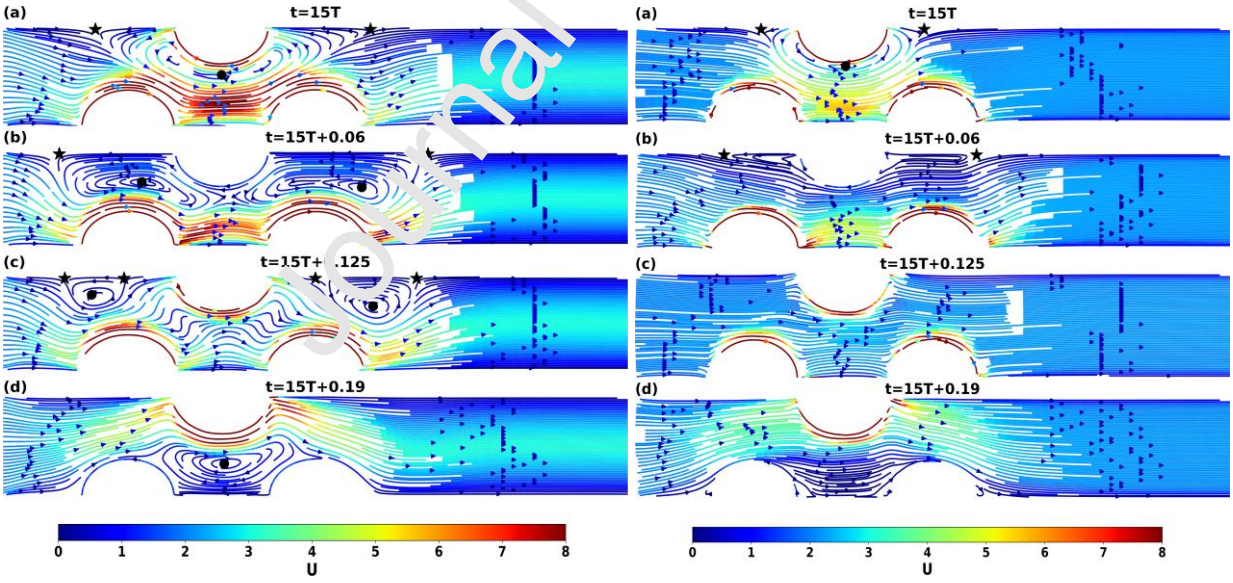

Figure 14. Exemplification of instantaneous flow patterns for the Newtonian case (left column) and Bn_{bulk}=26.5 (right column). The time instants are indicated in the top inserts of each panel.

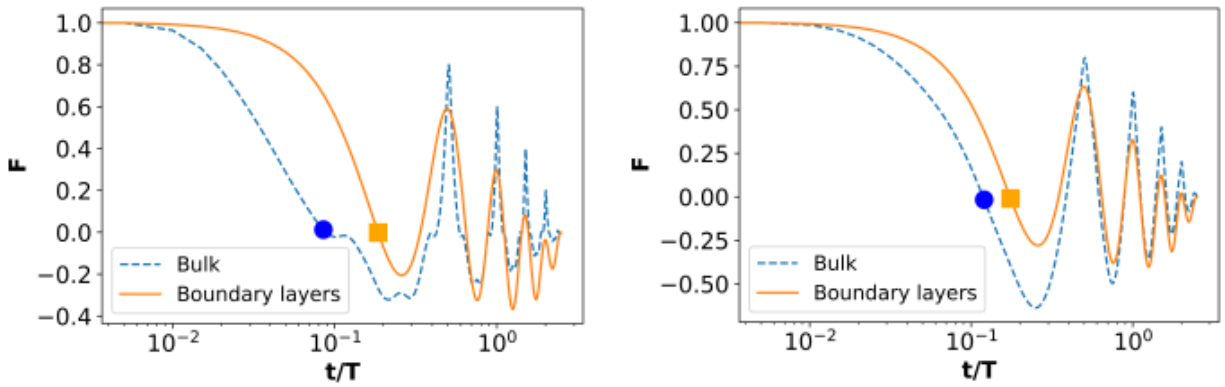

Figure 15. Time auto-correlation functions of the passive scalar fluctuations averaged within the mixing boundary layers (full lines) and within the bulk of the flow (dashed lines) computed for the reference Newtonian case –left panel and for the highest yield stress case explored, Bn_{bulk} = 26.5, N = 0.75 –right panel. In both panels the full symbols mark the first zero crossing of the auto-correlation functions which defines the characteristic time of correlation of the passive scalar fluctuations.

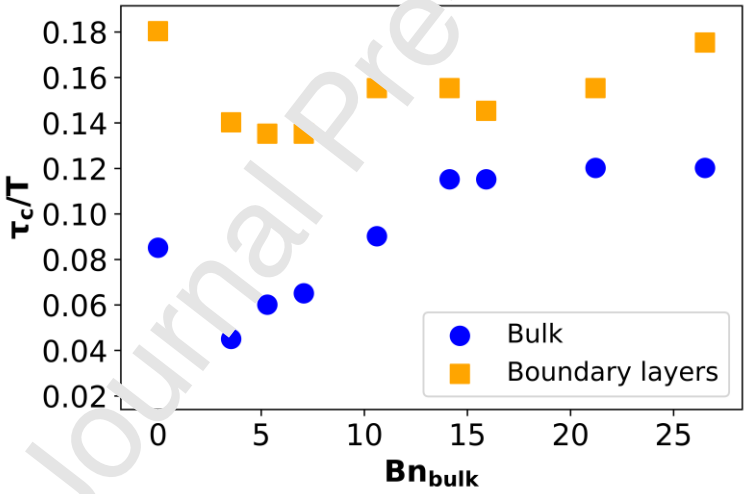

Figure 16. Dependence of the correlation times of the passive scalar fluctuations computed in the bulk of the flow (blue circles) and within the boundary layers (orange squares) on the bulk Bingham number Bn_{bulk}.

Figure 17. Illustration of un-yielded zones at Bnbulk = 26.5 and several time instants indicated in the top inserts. The solid blobs located within the "active "mixing zone and accounted for in the size statistics are highlighted by a red contour while the others are highlighted by a yellow contour.

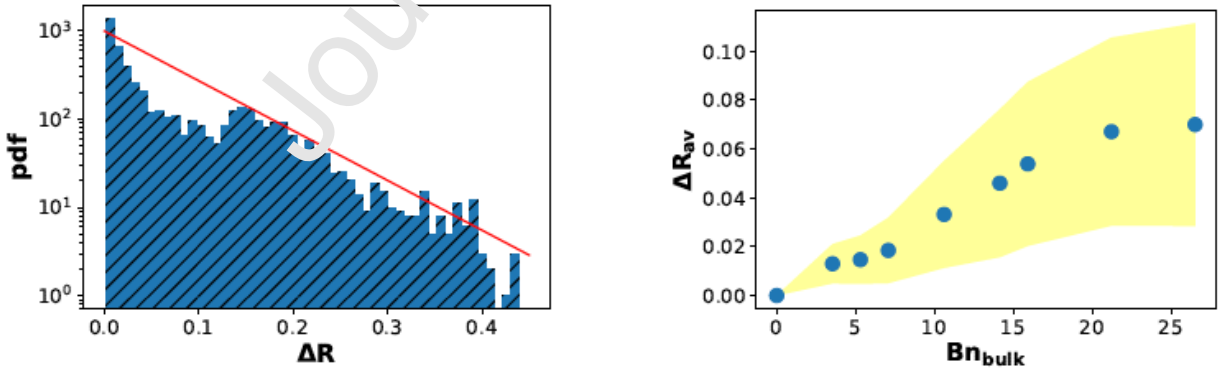

Figure 18. Size statistics of the un-yielded blobs in the active mixing region: left –probability distribution function (pdf), right –dependence of the mean size of the unyielded blobs R_{av} on the bulk Bingham number Bn_{bulk}.

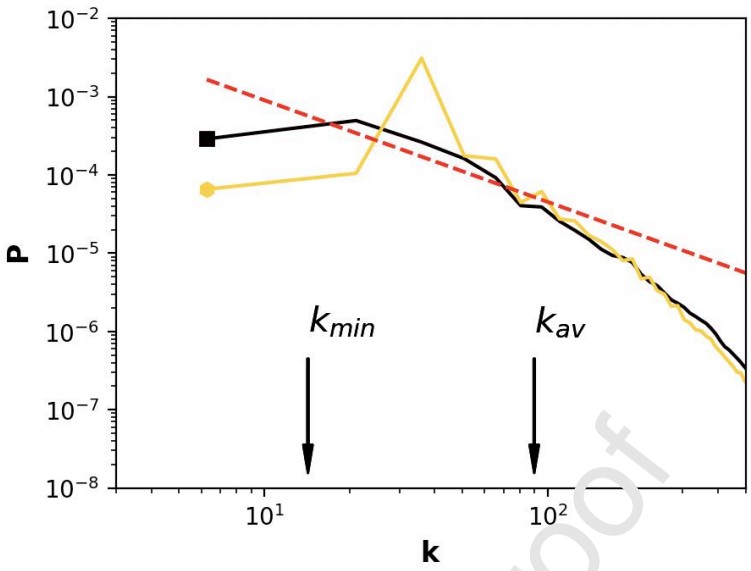

Figure 19. Spatial power spectra of the fluctuations of the passive scalar computed for the Newtonian reference case (the data set marked by a square) and for the largest yield stress case investigated. The dashed line is a guide for the eye, k^{-1}.

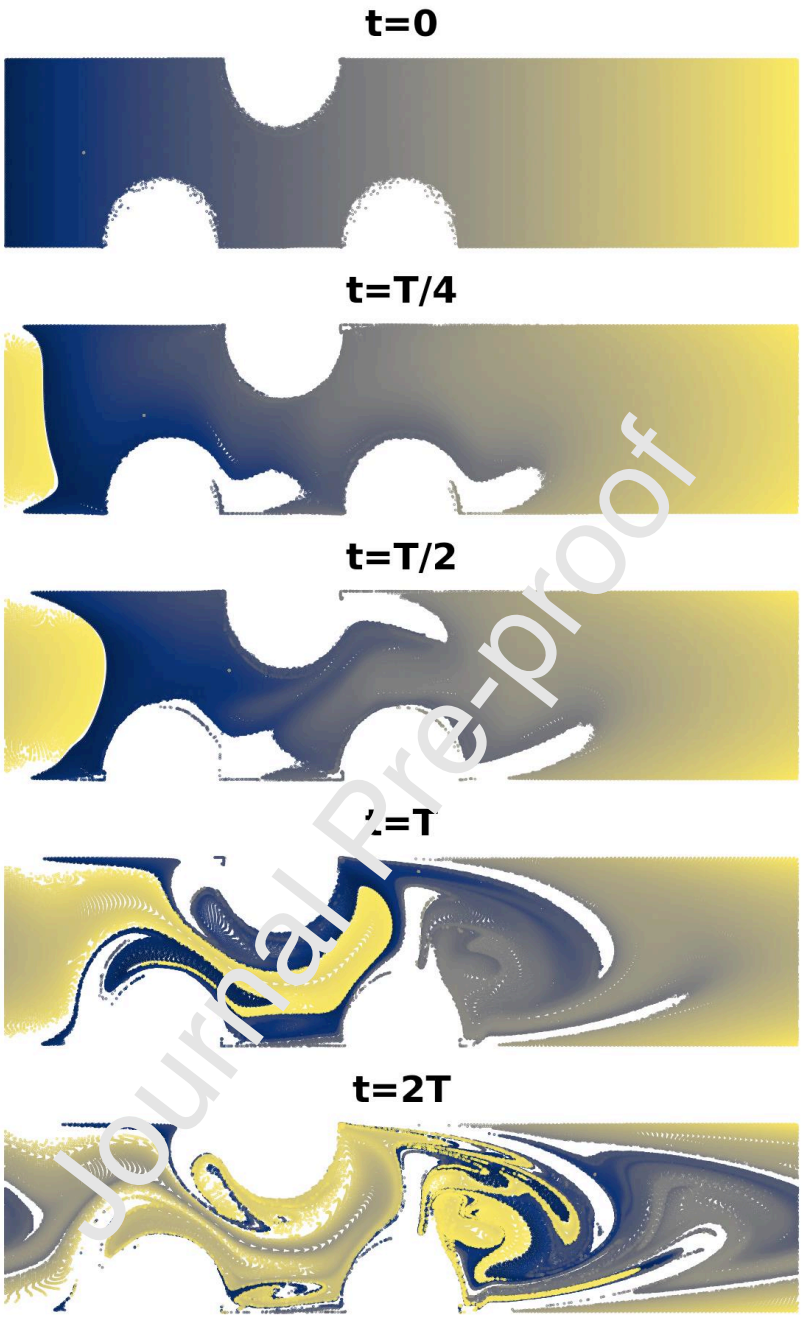

Figure 20. Instantaneous positions of Lagrangian tracers evenly distributed within the mixing channel at t = 0 at different time instants indicated in the top inserts. The false color map refers to the axial position x of the initial tracers. The data refer to the reference Newtonian case, Bn_{bulk} = 0, N = 1.

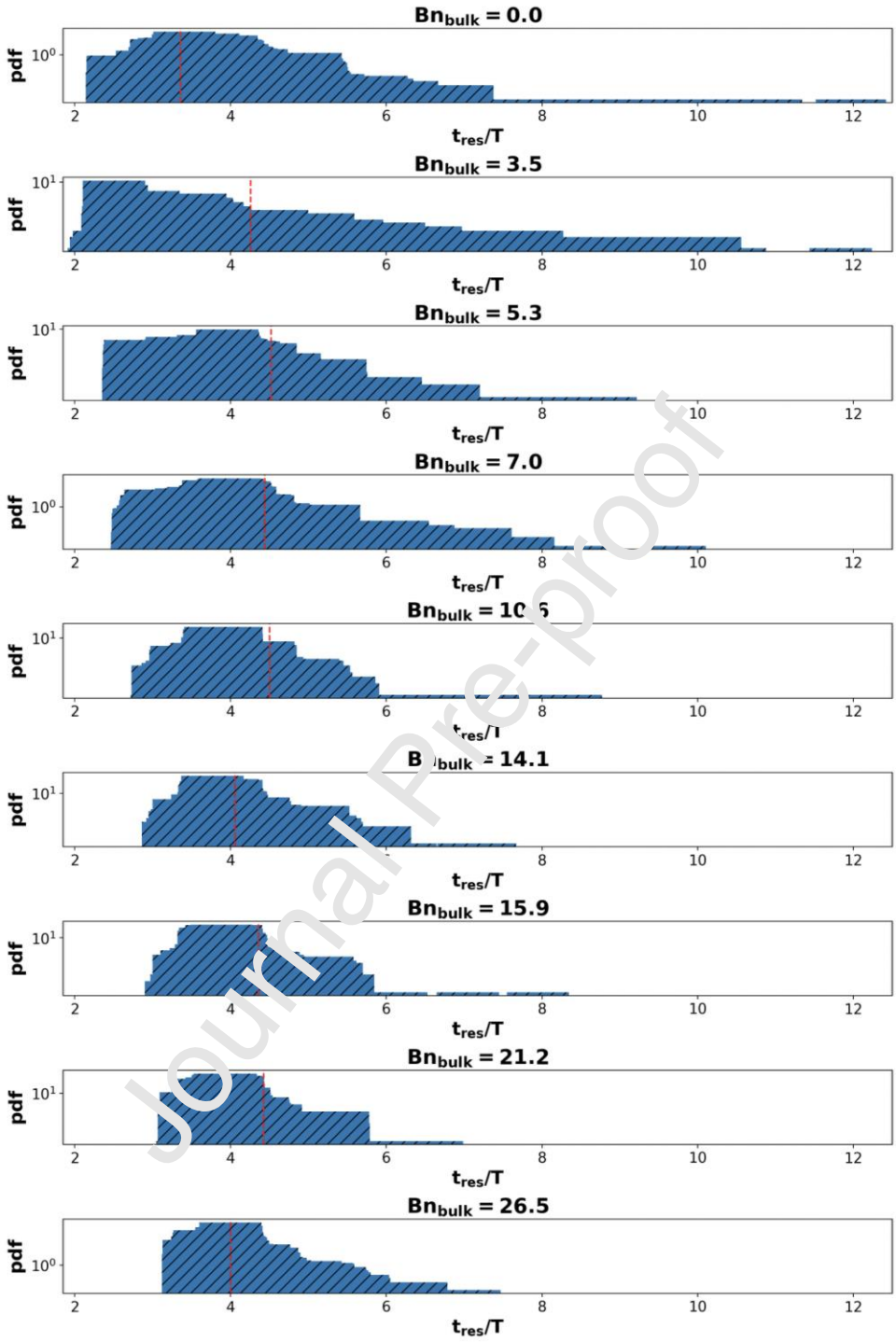

Figure 21. Histograms of the residence times for various bulk Bingham numbers Bn_{bulk} indicated in the top inserts. In each panel the vertical dashed line marks the reduced advection time t_a/T.

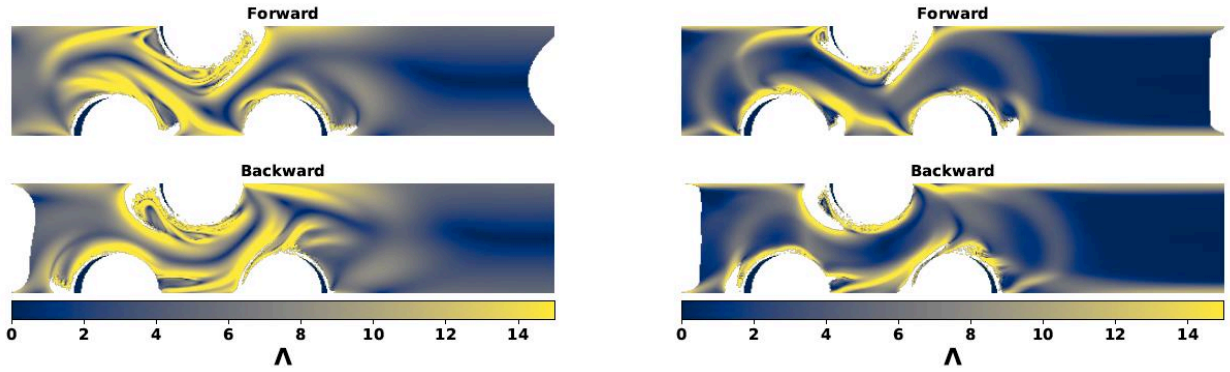

Figure 22. Maps of the forward and backward Lyapunov exponents obtained for the Newtonian case (left column) and Bn_{bulk}=26.5 (right column).

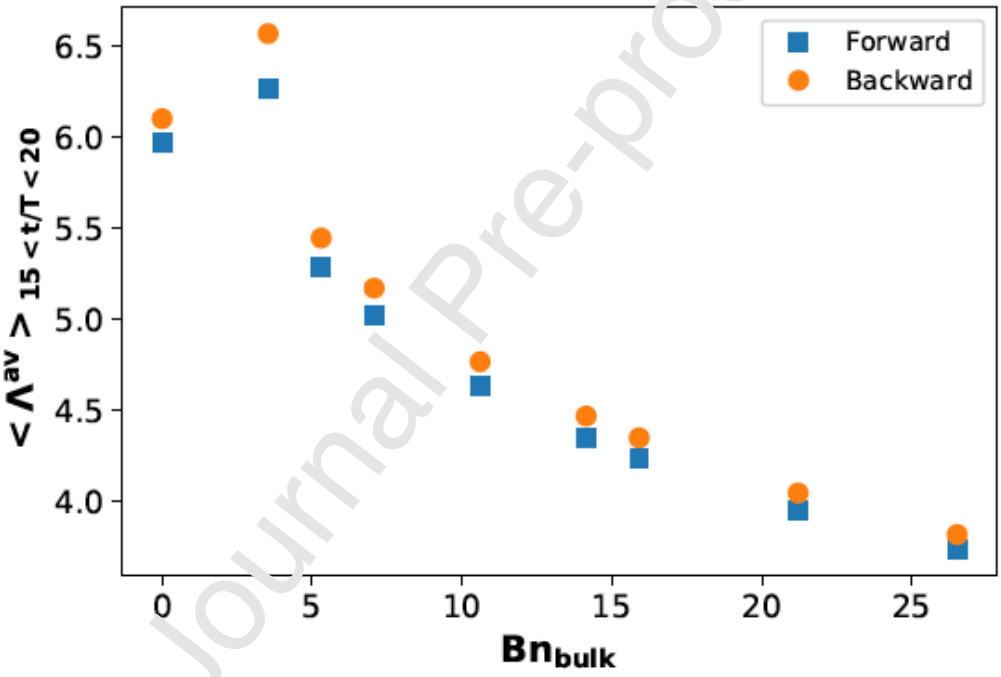

Figure 23. Dependence of the spaced averaged Lyapunov exponent averaged over the last five periods of the mixing process on the bulk Bingham number Bn_{bulk}.

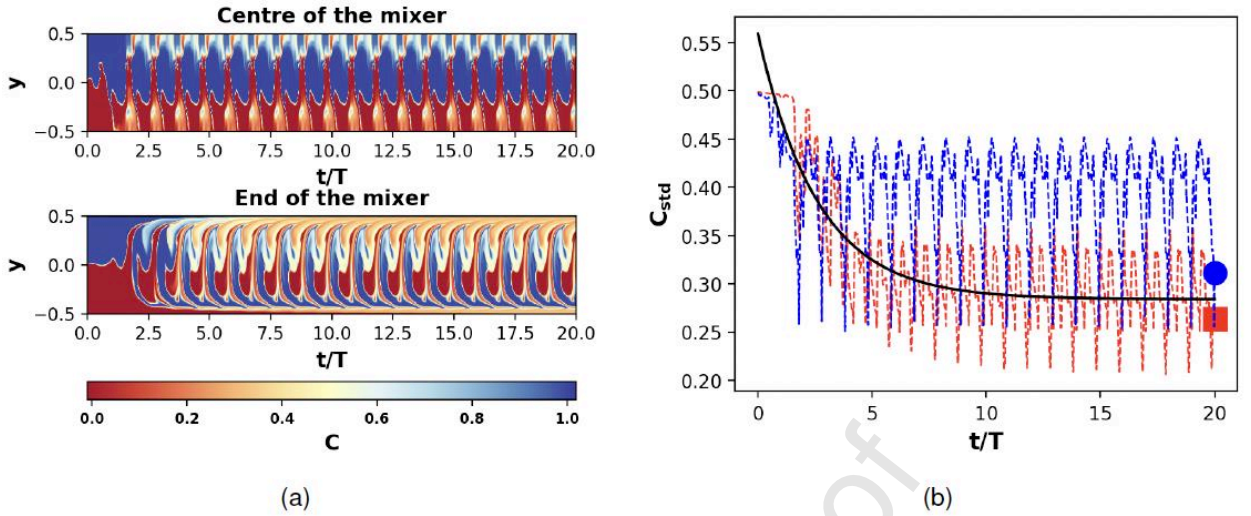

Figure 24. (a) Space time plots obtained for the highest yield stress case (Bn_{bulk} = 26.5, N = 0.75) at the centre of 4 rotating arc-walls mixer (top panel) and at its exit of the mixer (bottom panel). (b) Time series of the mixing indicator Cstd obtained for the highest yield stress case (Bn_{bulk} = 26.5, N = 0.75) at the centre of the mixer of the 4 rotating arc-walls mixer (circle) and at the exit of the mixer (square). The full line is an exponential fitting function.

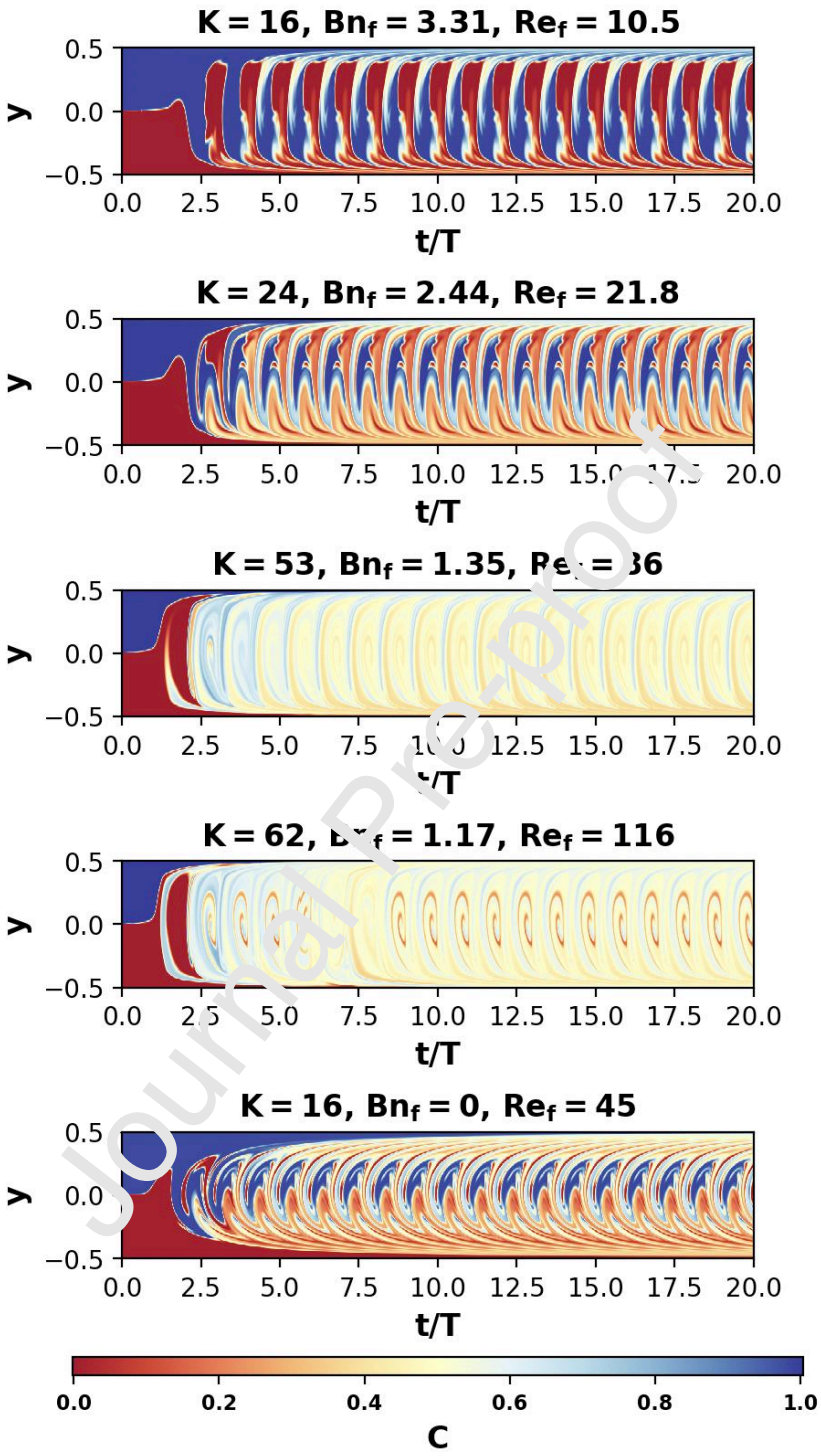

Figure 25. Space-time diagrams of the mixing process at the exit of the mixer for various forcing schemes summarized in the top inserts (see the text for the description of the numerical setting). The bottom panel refers to the reference Newtonian case already discussed through the manuscript.

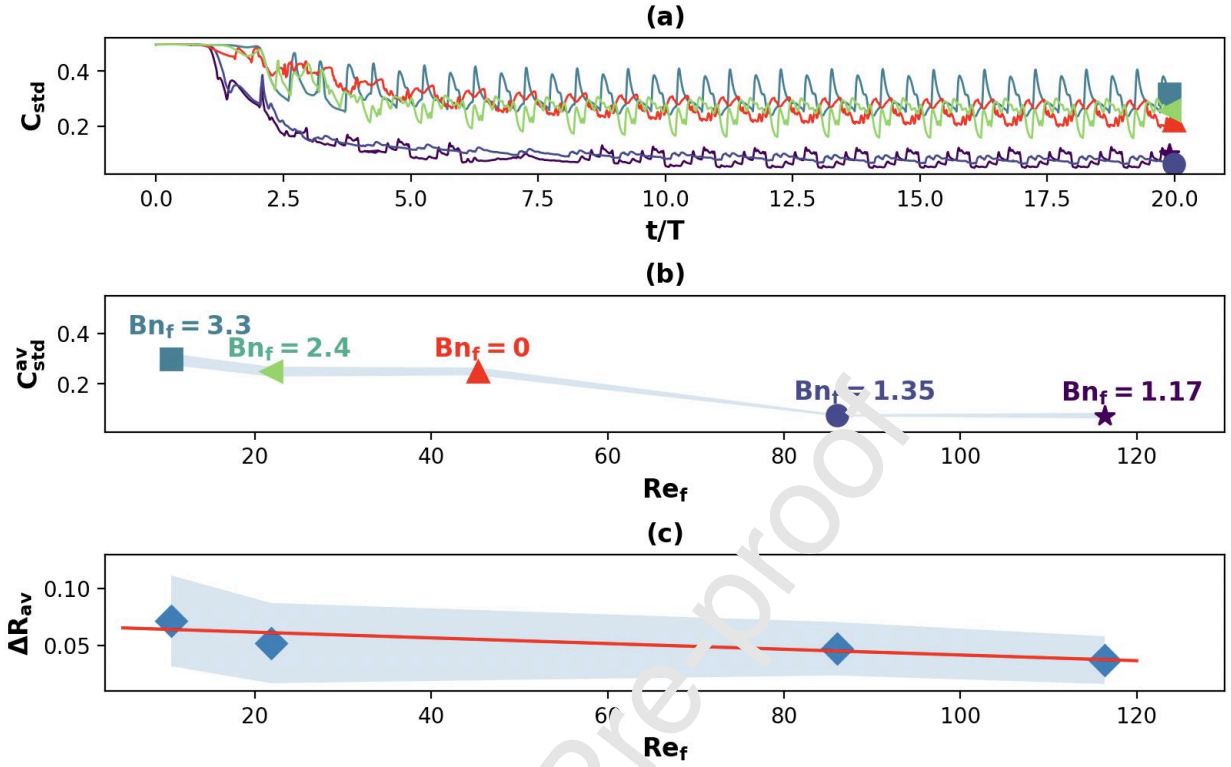

Figure 26. (a) Time series of the mixing indicator C_{std} obtained at the exit of the mixer for the forcing schemes illustrated in Fig. 30: (b) Dependence of the mixing efficiency parameter on the forcing Reynolds number Re_f. The corresponding forcing Bingham numbers Bnf are indicated in the text annotations. The shaded regions highlight the level of fluctuations of the mixing indicator around its time-averaged steady state value C^{av}_{std} (c) Dependence of the averaged size of the recirculation zone ΔR_{av} on the forcing Reynolds number Re_f for a fixed bulk Bingham number Bn_{bulk} = 26.5 and a fixed bulk Reynolds number Re_{bulk} = 0.05. The full line is a linear fit. In panels (a, b) the symbols refer to the parameters of the external forcing: square - K = 16, Bn_f = 3.3, Re_f = 10.5, left triangle - K = 24, Bn_f = 2.4, Re_f =21.8, circle-K=53, Bn_f =1.35, Re_f =86, star - K=62, Bn_f =1.17, Re_f =116, up triangle-K=16, Bn_f =0, Re_f =45.

CRediT author statement

N/A

Acknowledgments

- Yann Moguen (former postdoc at University of Pau)
- Yves Le Guer - University of Pau
- Kamal El Omari - University of Pau
- Eliane Younes (former PhD candidate in our group)
- Cathy Castelain

Funding: This work was supported by the French research Program No.
(Novel active inline Mixer for Yield Stress fluids, NaiMYS).

Declaration of interests

*Please **tick** the appropriate statement below and declare any financial interests/personal relationships which may affect your work in the box below.*

The authors declare that they have no known competing financial interests or personal relationships that could have appeared to influence the work reported in this paper.

The authors declare the following financial interests/personal relationships which may be considered as potential competing interests:

Please declare any financial interests/personal relationships which may be considered as potential competing interests here.

References

[1]. El Omari, Kamal, Younes, Eliane, Burghelea, Teodor, Castelain, Cathy, Moguen, Yann & Le Guer, Yves Active chaotic mixing in a channel with rotating arc-walls. Phys. Rev. Fluids 6, 024502, 2021.
[2]. Eliane Younes, Yann Moguen, Kamal El Omari, Teodor Burghelea, Yves Le Guer, Cathy Castelain, Experimental study of chaotic flow and mixing of Newtonian fluid in a rotating arc-wall mixer, International Journal of Heat and Mass Transfer, 187, 122459, 2022.
[3]. Younes, Eliane 2020 Nouveau mélangeur à advection chaotique pour les fluids visqueux newtoniens et à seuil, PhD thesis, Nantes 2020.
[4]. Yann Moguen, Eliane Younes, Kamal El Omari, Cathy Castelain, Yves Le Guer, Teodor Burghelea, Active chaotic mixing in a channel with rotating arc-walls, in preparation.

Further reading

[1] Batchelor GK (1959) Small-scale variation of convected quantities like temperature in turbulent fluid
part 1. general discussion and the case of small conductivity. J Fluid Mech 5(1):113 – 133.
[2] Burghelea T, Segre E, Bar-Joseph I, et al (2004a) Chaotic flow and efficient mixing in a microchannelwith a polymer solution. Phys Rev E 69(6):066,305 –8
[3] Gouillart E, Dauchot O, Dubrulle B, et al (2008) Slow decay of concentration variance due to no-slipwalls in chaotic mixing. Phys Rev E 78:026,211.
[4] Jullien, Castiglione, and Tabeling] Jullien MC, Castiglione P, Tabeling P (2000) Experimental observation of Batchelor dis- persion of passive tracers. Phys Rev Lett 85:3636 –3639.

[5] Lyapunov AM (1885) On the stability of ellipsoidal figures of equilibrium of a rotating fluid (in Russian). Bulletin Astronomique 1885.
[6] Popinet S (2003) Gerris: a tree-based adaptive solver for the incompressible Euler equations in complex geometries. J Comput Phys 190 (2):572–600.

Author Biography

Teodor Burghelea is a researcher with the Centre Nationale de la Recherche Scientifique (CNRS) at the Laboratoire de Thermique et Energie de Nantes, Nantes, France. His research interests are in non-Newtonian fluid mechanics and rheology. In particular he is interested in the fluid mechanics of yield stress materials.